Article

Developmental Cell

Absence of Radial Spokes in Mouse Node Cilia Is Required for Rotational Movement but Confers Ultrastructural Instability as a Trade-Off

Graphical Abstract

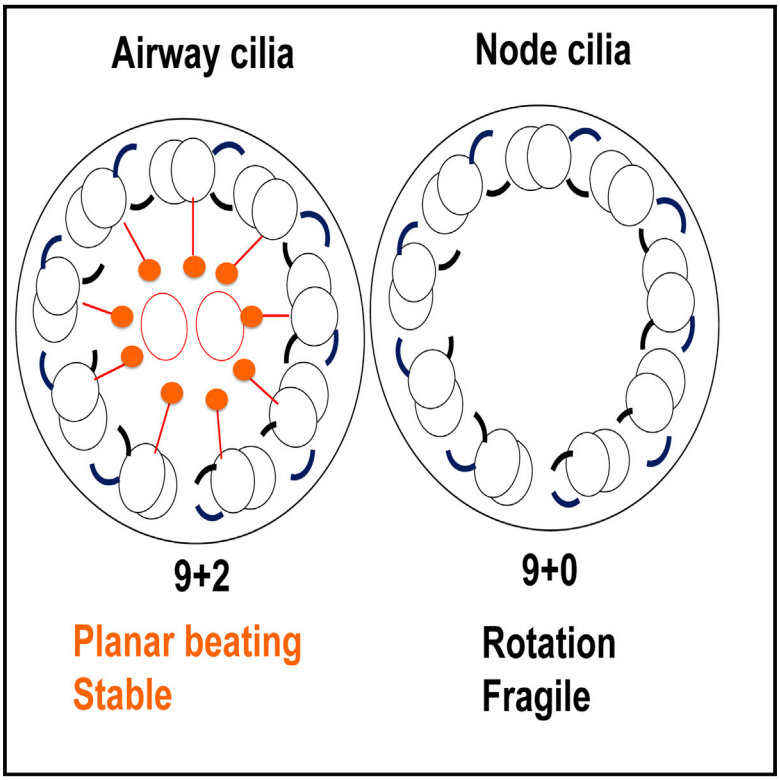

Authors

Kyosuke Shinohara, Duanduan Chen, Tomoki Nishida, Kazuyo Misaki, Shigenobu Yonemura, Hiroshi Hamada

Correspondence

k_shino@cc.tuat.ac.jp

In Brief

How do mammalian cilia sustain a specific pattern of motion? Shinohara et al. show that radial spokes in the ciliary microtubule structure are determinates of ciliary motion. Radial spokes maintain airway cilia beating motion, whereas their absence from node cilia allows for unidirectional rotation but renders them ultrastructurally fragile.

Highlights

- Mouse node cilia but not airway cilia are sensitive to microtubule destabilization
- Node cilia rotation requires a 9+0 doublet MT structure with no radial spokes
- Radial spokes are required to maintain an airway cilia 9+2 structure and beating motion
- Lack of radial spokes induces rotational motion but makes the MT ultrastructure fragile

Shinohara et al., 2015, Developmental Cell *35*, 236–246
October 26, 2015
http://dx.doi.org/10.1016/j.devcel.2015.10.001

CellPress

CellPress

Developmental Cell
Article

Absence of Radial Spokes in Mouse Node Cilia Is Required for Rotational Movement but Confers Ultrastructural Instability as a Trade-Off

Kyosuke Shinohara,[1,5,6,*] Duanduan Chen,[2,5] Tomoki Nishida,[3,5,7] Kazuyo Misaki,[4] Shigenobu Yonemura,[4] and Hiroshi Hamada[1]

[1]Developmental Genetics Group, Graduate School of Frontier Biosciences, Osaka University, Suita, Osaka 565-0871, Japan
[2]Department of Biomedical Engineering, School of Life Science, Beijing Institute of Technology, Beijing 100081, China
[3]Research Center for Ultra-high Voltage Electron Microscopy, Osaka University, Osaka 567-0047, Japan
[4]Ultrastructural Research Team, Center for Life Science Technologies, RIKEN, Kobe 650-0047, Japan
[5]Co-first author
[6]Present address: Department of Biotechnology and Life Science, Tokyo University of Agriculture and Technology, 2-24-16, Naka-machi, Koganei, Tokyo 184-8588, Japan
[7]Present address: Japan Textile Products Quality and Technology Center, 5-7-3, Shimoyamate-dori, Chuo-ku, Kobe-city, Hyogo-ken 650-0011, Japan
*Correspondence: k_shino@cc.tuat.ac.jp
http://dx.doi.org/10.1016/j.devcel.2015.10.001

SUMMARY

Determination of left-right asymmetry in mouse embryos is established by a leftward fluid flow that is generated by clockwise rotation of node cilia. How node cilia achieve stable unidirectional rotation has remained unknown, however. Here we show that brief exposure to the microtubule-stabilizing drug paclitaxel (Taxol) induces randomly directed rotation and changes the ultrastructure of node cilia. In vivo observations and a computer simulation revealed that a regular 9+0 arrangement of doublet microtubules is essential for stable unidirectional rotation of node cilia. The 9+2 motile cilia of the airway, which manifest planar beating, are resistant to Taxol treatment. However, the airway cilia of mice lacking the radial spoke head protein Rsph4a undergo rotational movement instead of planar beating, are prone to microtubule rearrangement, and are sensitive to Taxol. Our results suggest that the absence of radial spokes allows node cilia to rotate unidirectionally but, as a trade-off, renders them ultrastructurally fragile.

INTRODUCTION

Left-right (L-R) asymmetry of the mouse embryo is determined as a result of the onset of leftward fluid flow (nodal flow) in the node cavity at 8 days after fertilization (Hirokawa et al., 2006; McGrath et al., 2003; Nonaka et al., 1998; Tabin and Vogan, 2003; Tanaka et al., 2005). This leftward flow is generated by the rotational movement of node cilia, which are solitary motile structures that contain microtubules with dynein arms (Hirokawa et al., 2006). The direction of the flow is determined by a combination of two features of node cilia: their posterior tilt and their clockwise rotation. Clockwise rotation of posteriorly tilted cilia thus generates a leftward effective stroke and rightward recovery stroke near the surface of the cell (Cartwright et al., 2004; Nonaka et al., 2005; Okada et al., 2005). Recent evidence has shown that planar cell polarity signaling positions the basal body at the posterior side of the node cells, giving rise to a posteriorly tilted rotational axis of the cilia (Hashimoto et al., 2010; Song et al., 2010). How node cilia are able to sustain stable unidirectional rotation has remained unknown, however.

Mice possess two types of motile cilia. The 9+2-type cilia present in the airway, brain, and oviduct contain nine peripheral doublet microtubules with dynein arms, one pair of single microtubules at the center of the axoneme (central pair), and radial spokes that physically connect the peripheral microtubules to the central microtubules. These cilia exhibit planar beating and generate global directional fluid flow. In contrast, the 9+0-type motile cilia present in the node cavity of the mouse embryo possess nine doublet microtubules with dynein arms but lack the central microtubules and radial spokes (Hirokawa et al., 2006). The driving force of ciliary bending is generated by sliding of the dynein arms between the peripheral doublet microtubules (Fox and Sale, 1987; Summers and Gibbons, 1971). Numerous elegant studies have established that the central pair, radial spoke, and the dynein regulatory complex (DRC) or nexin play critical roles in regulating the beating pattern of *Chlamydomonas* flagella and sea urchin sperm (Brokaw, 2009; Lindemann, 1994, 2003; Satir et al., 2014). In *Chlamydomonas*, the central pair apparatus and radial spokes operate by mechanochemical signaling to regulate dynein activity (Oda et al., 2014; Smith and Yang, 2004). DRC or nexin is an elastic linker between doublet microtubules that functions as a signal transduction device of dynein regulation and as a local restriction device of interdoublet sliding (Gardner et al., 1994; Heuser et al., 2009; Lindemann et al., 2005). Mouse and human genetics have also revealed that the central pair, radial spoke, and DRC or nexin are critical for intact motility of cilia, and disruption of this motility causes primary ciliary dyskinesia (Antony et al., 2013; Becker-Heck et al., 2011; Burgoyne et al., 2014; Castleman et al., 2009; Knowles et al., 2014; Lechtreck et al., 2008; Lin et al.,

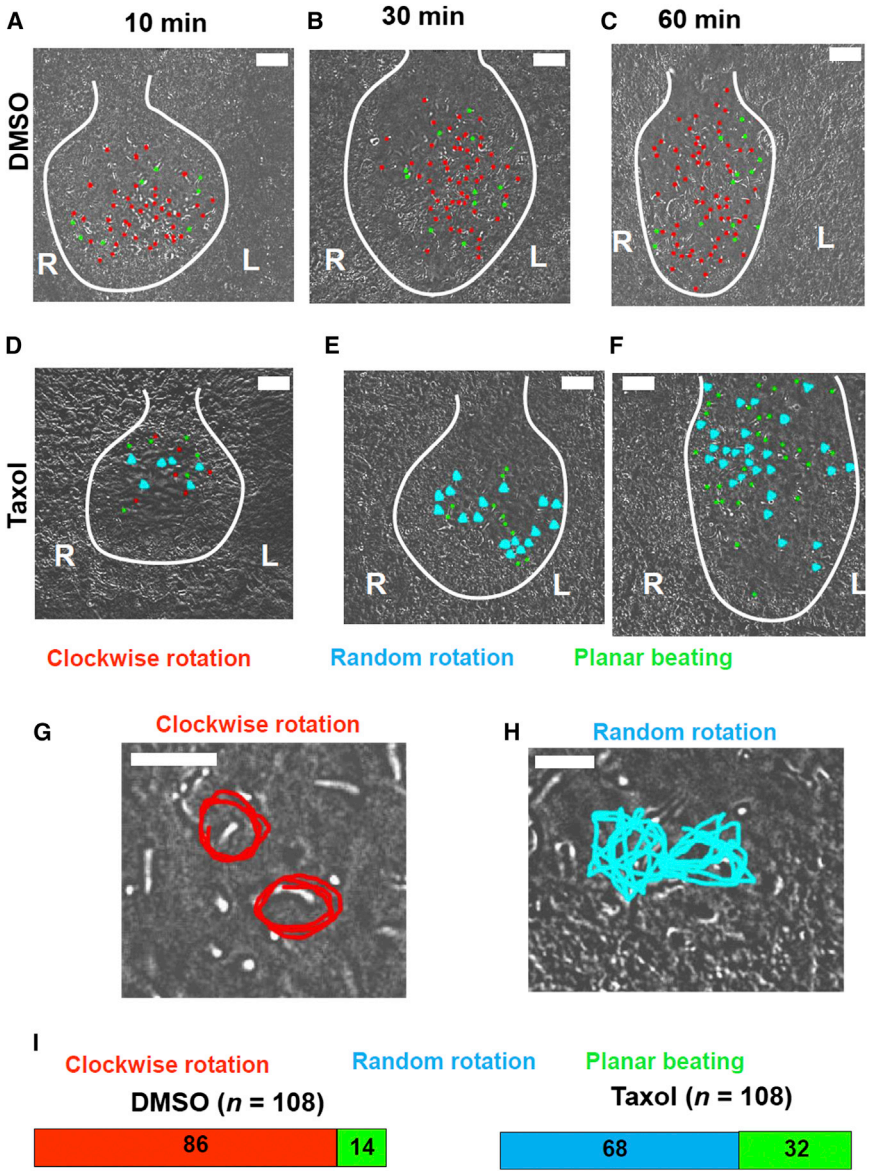

Figure 1. Taxol Randomizes the Rotation of Node Cilia

(A–F) Motion pattern of node cilia at various times after the onset of culture of mouse embryos in a medium containing a DMSO (0.1%) vehicle (A–C) or 5 μM Taxol (D–F) at 37°C. L and R denote the left and right sides of the embryo, respectively. White lines demarcate the node cavity. Red, blue, and green dots indicate cilia rotating in clockwise, those rotating in random directions, and those manifesting planar beating, respectively.

(G and H) Traces of ciliary tips engaged in stable clockwise rotation (G) or random rotation (H).

(I) Summary of the ciliary motion pattern in the node cavity of mouse embryos 1 hr after culture onset in the presence of DMSO or Taxol. Red, blue, and green bars denote the percentages of cilia manifesting the different motion patterns indicated in (A).

White size bars represent 10 μm (A–F) or 5 μm (G and H). A minor population (less than 1%) of node cilia shows random rotation in WT mouse embryos.

2014; Merveille et al., 2011). In contrast to numerous studies on the beating pattern of *Chlamydomonas* flagella and sea urchin sperm, however, the relation between ultrastructure and ciliary motion pattern remains to be elucidated in mammals.

We have examined the relation between ciliary geometry and motion of mouse motile cilia. Unexpectedly, we found that a chemical treatment markedly changed the arrangement of microtubules in motile cilia and that the radial spokes maintain the regular arrangement of these microtubules and determine the motion pattern of mouse cilia.

RESULTS

Taxol Treatment Randomizes the Rotational Movement of Node Cilia

Treatment of mouse embryos with various chemicals for examination of their ability to randomize the normally clockwise rotation of node cilia revealed that paclitaxel (Taxol), an anticancer drug that stabilizes microtubules (Boisvieux-Ulrich et al., 1989; Nogales et al., 1998; Sharma et al., 2011), impaired the clockwise rotation. Indeed, Taxol treatment for a short time gave rise to a pronounced change in the motion pattern of node cilia (Figures 1A–1H). In control embryos treated with a DMSO vehicle, >80% of cilia showed persistent clockwise rotation (Movie S1). In embryos treated with 5 μM Taxol, however, a substantial proportion (~30%) of node cilia showed random rotation (a motion pattern characterized by alternating clockwise and anticlockwise rotation that was not observed in nontreated node cilia) 10 min after treatment onset, with no cilia maintaining clockwise rotation at 30 min (Figures 1D–1F; Movie S1). After 1 hr of Taxol exposure, 68% of node cilia manifested random rotation, with none showing clockwise rotation (Figure 1I; Movie S1). The Taxol-induced random rotation of cilia was temperature dependent, being apparent at 37°C but not at lower temperatures, such as 25°C.

Taxol Treatment Disturbs the Regular Arrangement of Doublet Microtubules in Node Cilia

The length of node cilia remained normal at 10 min after Taxol treatment but increased at 60 min (Figure S1). We next examined the ultrastructure of node cilia. In Taxol-treated embryos, transverse sections of the axoneme revealed that the positioning of doublet microtubules was disorganized (15 of 15 cilia examined) (Figures 2A–2C) while outer dynein arms were retained. We adopted the term "transposition" to describe such abnormal microtubule positioning, with doublet microtubules changing

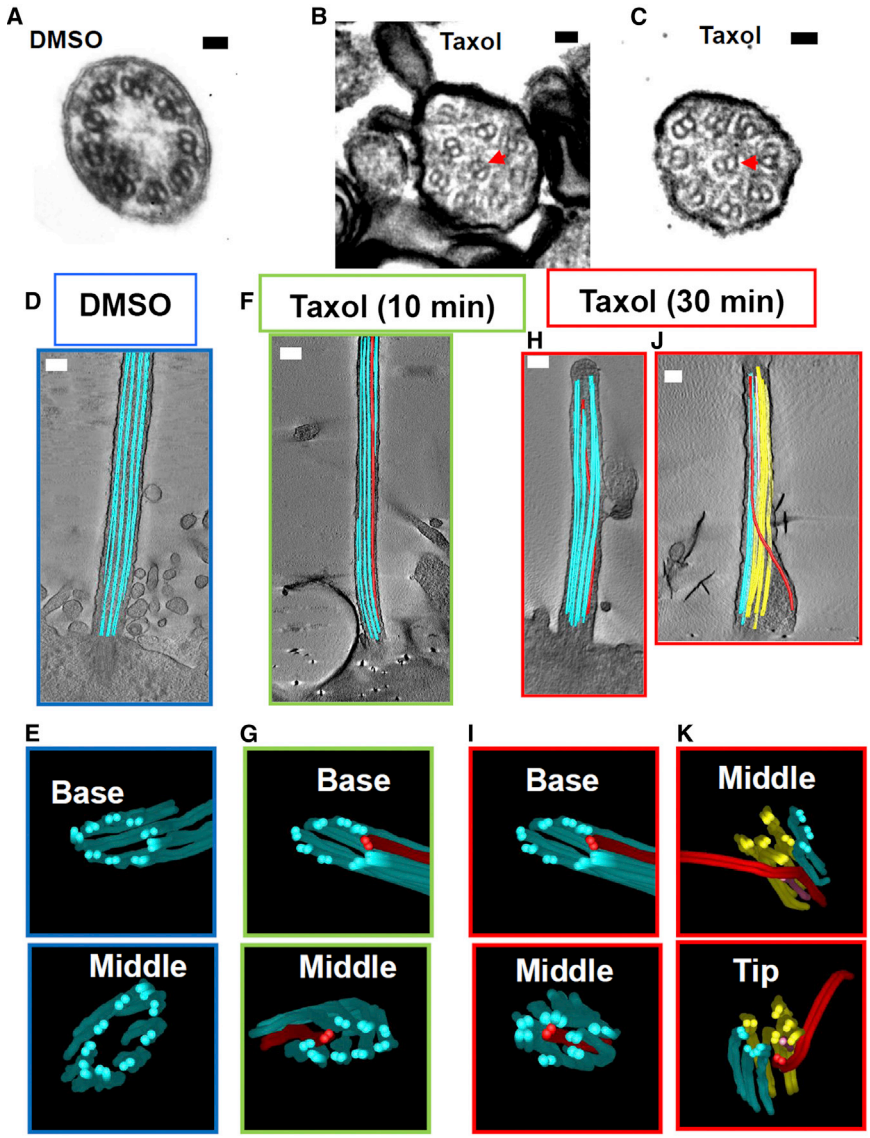

Figure 2. Disorganized Arrangement of Doublet Microtubules in Node Cilia of Taxol-Treated Embryos

(A–C) TEM of cross-sections of node cilia in mouse embryos treated with DMSO (A) or 5 μM Taxol for 30 min (B and C). Whereas a regular circular arrangement of nine doublet microtubules was apparent in control embryos, the arrangement of doublet microtubules was disorganized (although dynein arms were retained) in Taxol-treated embryos. Red arrowheads indicate doublet microtubules that have undergone transposition.

(D–K) Electron tomography of doublet microtubules in node cilia of embryos cultured with DMSO for 30 min (D and E, blue panels) or with 5 μM Taxol for 10 min (F and G, green panels) or 30 min (H–K, red panels). Doublet microtubules that are present in the normal position, that shift their position from the periphery to the center of the axoneme, or that remain at the center of the axoneme within the region of observation are shown in blue, red, and yellow, respectively. The lower panels show the arrangement of doublet microtubules at the base, middle, and tip of the axoneme.

Black and the white size bars represent 50 nm (A–C) and 0.2 μm (D, F, H, and J), respectively. See also Figures S1–S3.

their position and invading from the periphery to the center of the axoneme. We further examined the three-dimensional structure of node cilia by electron tomography with an ultra-high-voltage electron microscope (Kunimoto et al., 2012). In control embryos cultured with DMSO for 30 min, node cilia maintained the regular arrangement of doublet microtubules from the basal region to the tip of the axoneme (Figures 2D and 2E; Movie S2). However, the arrangement of microtubules was greatly disorganized at the middle segment of the axoneme in embryos treated with Taxol for 30 min (Figures 2H–2K; Movie S2). Treatment with Taxol for only 10 min induced randomized motion in a small proportion of node cilia (Figure 1D), and this effect was accompanied by mild transposition, with only one microtubule doublet being affected in 3 of 4 cilia examined (Figures 2F and 2G). Transposition of one pair of microtubules took place not at the basal region but in the middle segment of the axoneme in 11 of 11 cilia examined. These results suggested that doublet microtubules of node cilia are unexpectedly dynamic.

The Regular Arrangement of Doublet Microtubules Is Essential for Stable Unidirectional Rotation of Node Cilia

Our results suggested that the spatial arrangement of doublet microtubules is an important determinant of ciliary motility pattern, but it is not possible experimentally to correlate structure and motion pattern for individual cilia. Computer simulation is a powerful approach to address the principle of ciliary motility. Brokaw has established several models that can reconstruct the beating pattern of cilia or flagella and has suggested a mechanism of axonemal dynein activation (Brokaw, 2002, 2005, 2009). For instance, to reconstruct a three-dimensional helical bending wave, axonemal dynein was proposed to work as both curvature sensors and motors, and its activation is regulated by local curvature of the doublet microtubule (Brokaw, 2002). In addition, a possible role of axonemal chirality in the stability of the rotational direction of cilia was proposed by the mathematical model (Hilfinger and Jülicher, 2008).

In this paper, we wished to address a separate issue, a relation between the ciliary motion pattern and the geometry of doublet microtubules. We therefore reconstructed realistic models of ciliary ultrastructure based on segmentation of corresponding electron tomography data and simulated the dynein-driven ciliary motion using the deformable mesh computer technique (Chen et al., 2011, 2014) (Figure 3A; see Supplemental Experimental Procedures). This method, to the best of our knowledge, is the first one that can predict ciliary motion based on electron tomography-reconstructed models. It provides more realistic

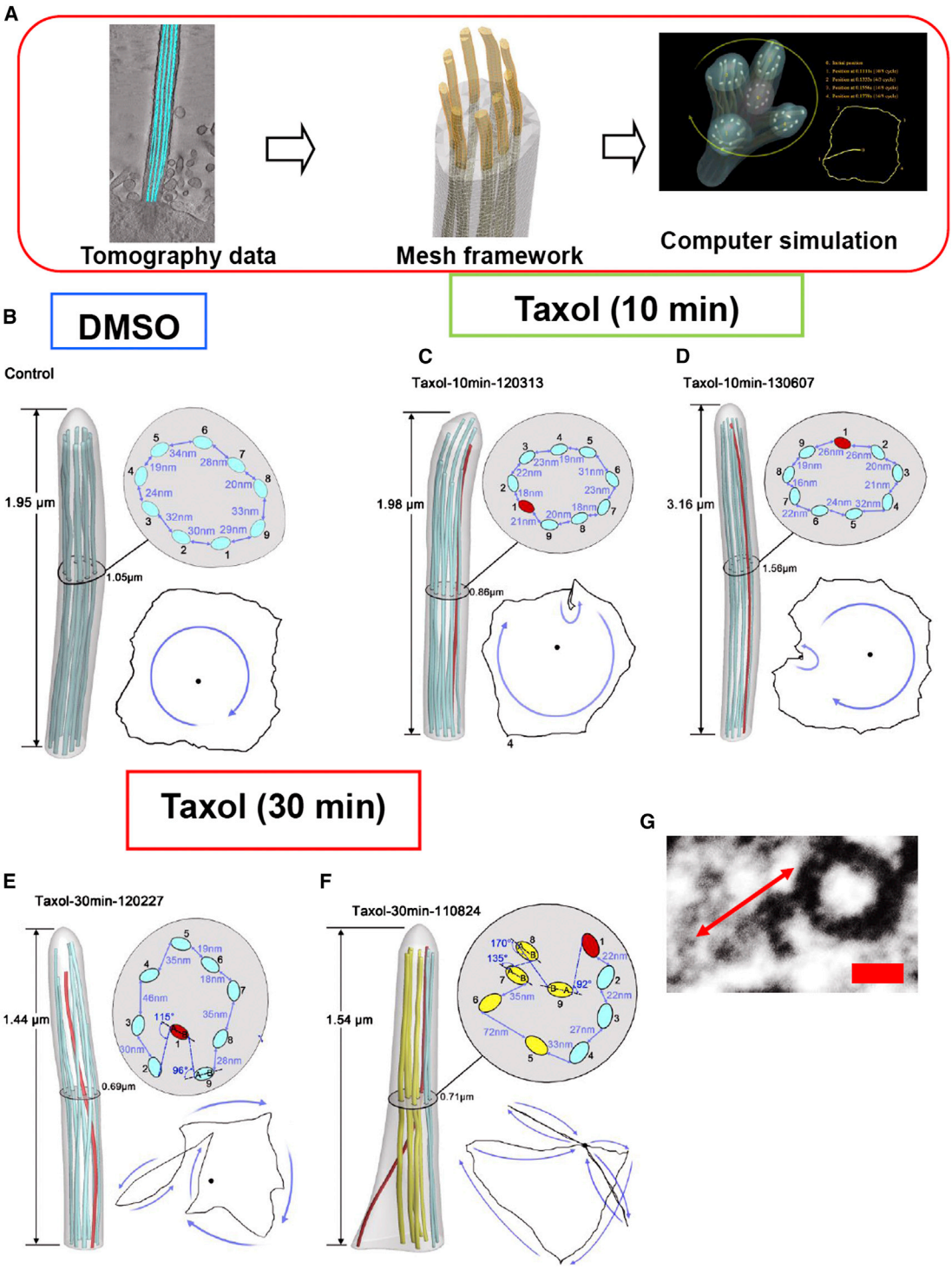

Figure 3. Computer Simulation of the Motion of Node Cilia

(A) Work flow of the computer simulation. A mesh framework of doublet microtubules was designed based on experimental data obtained by electron tomography. The dynein arm-driven deformation of the axoneme was calculated with a finite element method.

(B–F) Traces of ciliary tip motion. Ciliary motion was calculated for embryos treated with DMSO for 30 min (B) or with 5 μM Taxol for 10 min (C and D) or 30 min (E and F). Typical cross-sections of the axoneme showing interdoublet distances are presented. Colored doublet microtubules correspond to the electron tomography data in Figure 2.

(G) TEM of an outer dynein arm of a node cilium showing the presence of two heads. The arrow indicates the length of the outer dynein arm. Red size bar represents 20 nm.

See also Figures S2 and S3.

modeling of the ciliary ultrastructure and, more importantly, allows us to study the relation between the ciliary motion pattern and the geometry of doublet microtubules for individual cilia. Given that node cilia possess outer dynein arms but lack inner dynein arms (Figure 2A), we assumed that sliding of the outer dynein arms induces deformation of the axoneme (Figures 3B–3F). Because the outer dynein arms are attached only to A tubules (Nicastro et al., 2006; Takada and Kamiya, 1994), effective establishment of dynein bridges is assumed to be determined by two factors—the interdoublet distance and the orientation of the doublet microtubules (A-B tubule polarity). We found that node cilia possess outer dynein arms with two heads (Figure 3G). Given that the mean length of the outer dynein arms of node cilia was 51.1 nm in our electron micrographs (Figure 3G, n = 18), we assumed that sliding of the dynein would occur between a pair of doublet microtubules only when they were separated by a distance of <50 nm. In a control cilium in which nine pairs of microtubules are aligned with the correct A-B polarity, the activation of dynein arms occurs unidirectionally (Movie S3; see Supplemental Experimental Procedures for details of the dynein activation pattern), resulting in clockwise rotation (Figure 3B). In contrast, in a cilium with transposition of doublet microtubules induced by treatment with Taxol for 30 min (Figure 3F), sliding of the dynein fails to occur between doublet microtubules 5 and 6, 8 and 9, and 9 and 1 below a height of 0.71 μm, as well as between doublets 4 and 5 below a height of 0.52 μm, because the interdoublet distance is >50 nm. Moreover, the orientation of the A-B tubules is disrupted in doublet microtubules 6 to 9. The sliding force thus produced clockwise or anticlockwise rotation, beating, or temporary suspension of ciliary motion (Figure 3F; Movie S3). The bending direction was uniform in the lower portion of the cilium, but it changed gradually in the upper portion as a result of the disrupted geometry of the sliding doublets. The overall ciliary movement therefore exhibited a disoriented whirling pattern. Treatment of mouse embryos with Taxol for 10 min resulted in mild transposition of microtubules in node cilia (Figures 2F and 2G), and the computer simulation revealed that transposition of even a single microtubule doublet renders node cilia unable to maintain stable clockwise rotation (Figures 3C and 3D), suggesting that the regular interdoublet distance and the orientation of doublet microtubules are essential for sliding of the dynein arms and unidirectional rotation. The stress distributions along the microtubules at particular snapshots during ciliary movement (Figure S2) suggested that the A-B tubule polarity influences the acting direction of the dynein force generating the moving pattern of a cilium.

Taxol Treatment Does Not Affect the Regular 9+2 Arrangement of Doublet Microtubules in Airway Cilia

Given that determination of L-R asymmetry is a robust event in vertebrates (Nakamura and Hamada, 2012), our finding that the architecture of node cilia is fragile and susceptible to perturbation was unexpected. To investigate the origin of this vulnerability of node cilia, we next examined the effects of Taxol treatment on the motion and structure of 9+2 motile cilia of the airway. Unlike node cilia, airway cilia harbor a pair of single microtubules and radial spokes at the center of the axoneme (Hirokawa et al., 2006). Treatment of airway tissue from mice with 5 μM Taxol for 2 hr had no effect on the motion or ultrastructure of the airway cilia. All cilia thus maintained planar beating in both DMSO-treated and Taxol-treated tissue (n = 133 and 218 cilia, respectively) (Figures 4A–4C; Movie S4). The regular circular arrangement of doublet microtubules was also maintained in all cilia of airway tissue treated with DMSO or Taxol (n = 314 and 268 cilia, respectively) (Figures 4D–4F). These results suggested that 9+2 motile cilia of the airway are resistant to Taxol treatment.

Absence of Radial Spokes Allows Rotational Movement but Renders the Arrangement of Doublet Microtubules Prone to Perturbation

Previous studies have shown that radial spokes play an important role in the motility of *Chlamydomonas* cilia through physical contact with the central pair of microtubules (Oda et al., 2014; Smith and Yang, 2004), but their precise role in mammalian cilia has remained elusive. Node cilia, which lack radial spokes, exhibit rotational movement and are sensitive to Taxol, whereas 9+2 airway cilia manifest planar beating and are resistant to Taxol. However, some node cilia of the wild-type (WT) mouse embryo show irregular beating, albeit at a low frequency (~1 of 200 cilia) (Figure 1; Movie S5). Consistently, transposition of doublet microtubules was found in a minor population of WT node cilia (2 of 40 cilia; Figure S3), while transposition was never detected in airway cilia of the WT mouse (0 of 113 cilia). We therefore hypothesized that radial spokes determine the motion pattern of cilia and stabilize the regular arrangement of doublet microtubules. To explore this hypothesis, we generated mice that lack the *Rsph4a* gene (Figure S4), an ortholog of *Rsp4*, which encodes the head of the radial spoke in *Chlamydomonas* (Pigino et al., 2011).

Rsph4a$^{-/-}$ mice were born without apparent L-R anomalies, and their node cilia showed normal rotational movement (Figures 5A and 5B; Movie S6). Conventional electron microscopy confirmed that the airway cilia of *Rsph4a*$^{-/-}$ mice lacked the head of the radial spoke (Figures 5C–5F). Importantly, most airway cilia of the mutant mice showed clockwise rotation instead of planar beating (Figures 6A–6C; Movie S6), consistent with recent observations in patients with primary ciliary dyskinesia (Burgoyne et al., 2014; Chilvers et al., 2003; Knowles et al., 2014). Radial spoke-deficient airway cilia thus mimicked the motion of node cilia. A substantial proportion (18%) of airway cilia in *Rsph4a*$^{-/-}$ mice also showed transposition of doublet microtubules, which was not detected in any airway cilia of WT mice (Figures 6D–6H), suggesting that the lack of radial spokes renders airway cilia prone to such transposition. In addition to transposition, the central pair of microtubules was lost in 12% of airway cilia in *Rsph4a*$^{-/-}$ mice (Figure S5), similar to patients with *RSPH1* mutations (Onoufriadis et al., 2014). Loss of normal radial spoke head tethering may induce instability or agenesis of the central microtubules.

Most airway cilia of *Rsph4a*$^{-/-}$ mice showed clockwise rotation when incubated with DMSO for 30 or 120 min (Figures 7A and 7B; Movie S4). However, a substantial proportion of these cilia (~10%) showed random rotation after incubation with 5 μM Taxol for 30 min (Figure 7C), and most of them (56%) did so after exposure to Taxol for 120 min (Figures 7D–7G; Movie S4). In addition, 52% of cilia (n = 91) showed transposition of

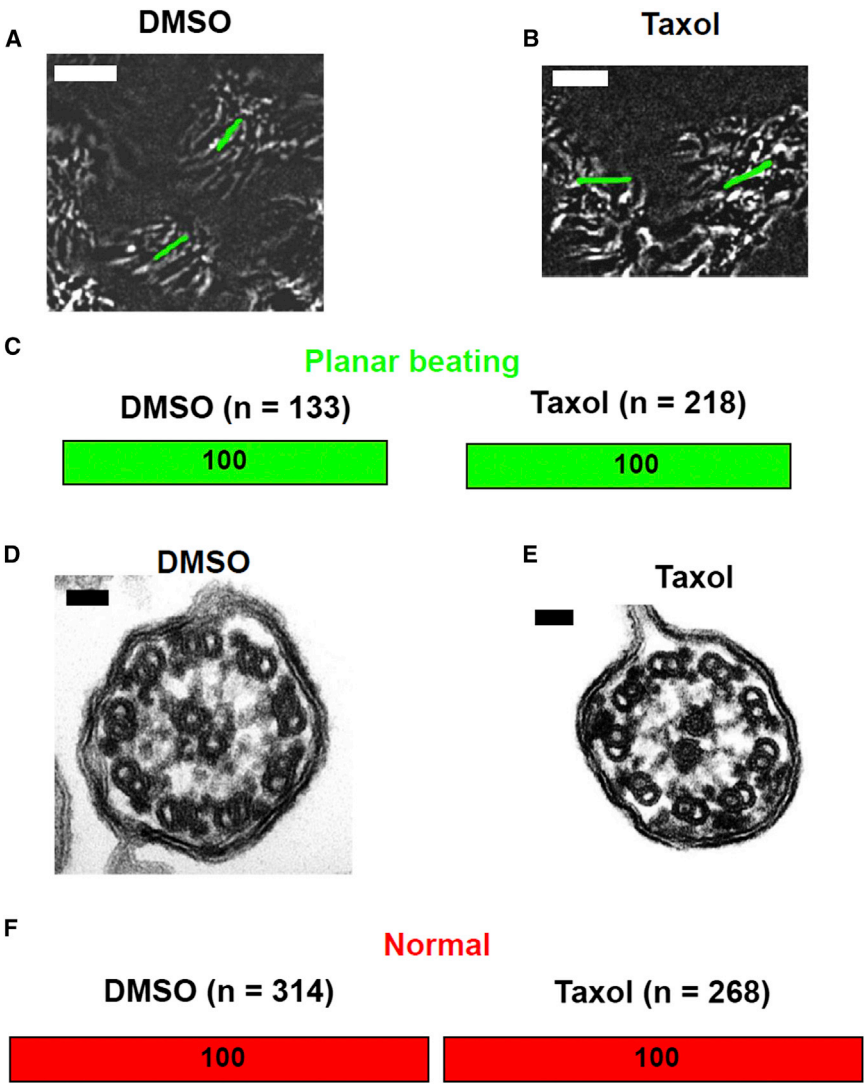

Figure 4. Taxol Does Not Affect the Motion or Arrangement of Doublet Microtubules in Airway Cilia

(A and B) Motion of cilia in mouse airway tissue cultured for 2 hr with DMSO (A) or 5 μM Taxol (B). Taxol-treated cilia maintained planar beating similar to that apparent for DMSO-treated cilia.

(C) Summary of the motion pattern of airway cilia. Green bars denote the percentage of cilia showing planar beating.

(D and E) TEM of cross-sections of airway cilia in tissue cultured as in (A) and (B). Taxol-treated cilia maintained a regular circular arrangement of doublet microtubules similar to that of DMSO-treated cilia.

(F) Summary of the organization of doublet microtubules. Red bars denote the percentage of cilia with a regular arrangement of doublet microtubules.

White and black size bars indicate 5 μm (A and B) and 50 nm (D and E), respectively.

doublet microtubules after incubation of *Rsph4a*$^{-/-}$ mouse airway tissue with Taxol for 2 hr, compared with only 12% for those (n = 63) exposed to DMSO (Figures 7H–7K). These results suggested that radial spokes are essential for the planar beating-type motion of 9+2 airway cilia and are required to maintain the regular arrangement of microtubules in motile cilia exposed to Taxol.

DISCUSSION

Our data obtained with two types of mouse motile cilia suggest that those of the node possess the ability to rotate unidirectionally as a result of the lack of radial spokes and possibly the central pair of microtubules. This lack of radial spokes, however, renders motile node cilia prone to structural perturbation. We found that some airway cilia of *Rsph4a*$^{-/-}$ mice show transposition of axonemal microtubules, as do those of primary ciliary dyskinesia patients with mutations of the *RSPH4A* gene (Burgoyne et al., 2014). Such microtubule instability may arise from the lack of mechanical interaction between radial spoke heads and central pair apparatus (Oda et al., 2014). Similar transposition has been occasionally detected in node cilia of mutant mice with an abnormal axonemal structure, such as *Pitchfork* mutant mice (Kinzel et al., 2010), and is found in a minor population of node cilia in the WT mouse (this study). Also in the DRC mutant, transpositions of doublet microtubules are observed, suggesting that DRC or nexin is another geometry-limiting factor in mammalian motile cilia (Becker-Heck et al., 2011; Merveille et al., 2011). Furthermore, it has remained unclear why node cilia have a 9+0 structure even though components of radial spokes (such as Rsph9) are expressed in the node of mouse embryos (Castleman et al., 2009). Unidentified proteins required for formation of the central pair of microtubules may thus be absent in these cilia.

Motile cilia with the 9+0 configuration exhibit rotational movement. Eel sperm, for example, show rotational motion and coincidentally lack radial spokes (Woolley, 1997, 1998). These findings, together with our observations of Rsph4a-deficient airway cilia, suggest that radial spokes likely function not only as a geometry-limiting device but also as a determinant that changes ciliary motion from rotation to planar beating. However, there may be inter-species differences among vertebrates in the structure and motility pattern of L-R organizer cilia. L-R organizer cilia in the fish and rabbit exhibit rotational movement (Kramer-Zucker et al., 2005; Okada et al., 2005), but mouse node cilia seem stiffer than zebrafish cilia. Both 9+0 and 9+2 cilia have been detected in the Kupffer's vesicle of the zebrafish embryo (Ferrante et al., 2009; Kramer-Zucker et al., 2005), while only the 9+0 type was reported in the Kupffer's vesicle of the medaka embryo (Okada et al., 2005; Omran et al., 2008). In the rabbit embryo, 9+0 and 9+2 cilia are found in the L-R organizer (Feistel and Blum, 2006). However, it is not clear whether the central pair of

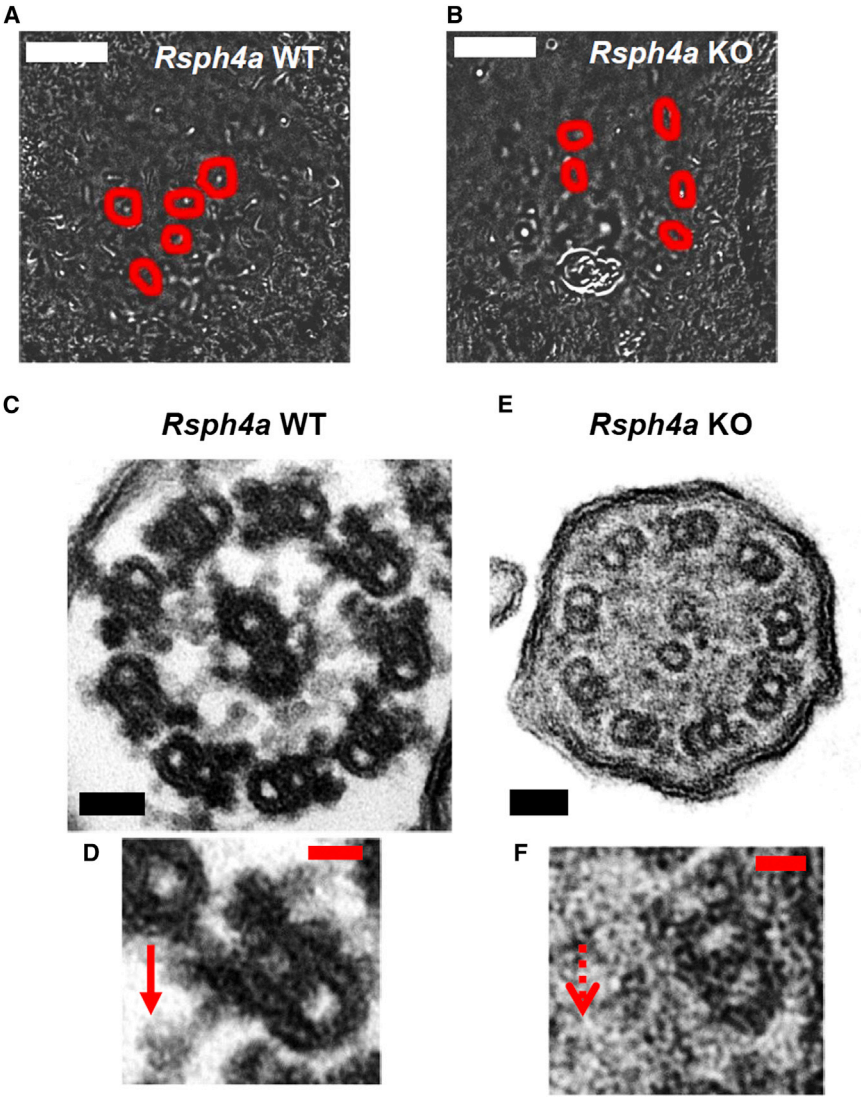

Figure 5. Typical Ultrastructure of Airway Cilia in WT and *Rsph4a* Knockout Mice

(A and B) Motion of node cilia in WT (A) and *Rsph4a*$^{-/-}$ (knockout, or KO) (B) mouse embryos. The clockwise rotation of node cilia was retained in the *Rsph4a*$^{-/-}$ mouse embryo.

(C–F) TEM of cross-sections of airway cilia in WT (C and D) and *Rsph4a*$^{-/-}$ (E and F) mice. The radial spoke head of the cilia apparent in WT mice (D, solid arrow) was missing from *Rsph4a*$^{-/-}$ mice (F, dotted arrow).

White, black, and red size bars indicate 20 μm (A and B), 50 nm (C and E), and 20 nm (D and F), respectively.

microtubules found in these 9+2 cilia is associated with radial spokes.

Strictly speaking, the planar beating of airway cilia is longitudinally compressed rotation (Ueno et al., 2012), but how radial spokes markedly distort the trace of rotation is unclear. It has been suggested that the radial spoke and the central pair manage transverse forces that act on the doublet microtubules (Lindemann, 1994, 2003). We also assume that the transverse forces are critical determinants of the motion pattern of mouse motile cilia and the radial spokes maintain intact dynamic distribution of the transverse forces. Given that radial spoke head-deficient cells are paralyzed in *Chlamydomonas* (Oda et al., 2014), the function of radial spokes may differ among species. Investigation of the precise structure and geometry of mouse motile cilia by cryoelectron microscopy may shed light on this issue. Although the precise function of mouse radial spokes is unknown, our data suggest that the architecture of node cilia is fragile as a result of the lack of radial spokes. Translation of the already-established anterior-posterior polarity to the L-R polarity in mouse embryos requires rotating cilia, because planar beating cilia would be unable to drive leftward flow. It would be of interest to know how vertebrate L-R organizers have acquired during evolution motile cilia that lack radial spokes.

It is not clear how Taxol induces transposition of microtubules after such short exposure periods. Microtubule plus-end tracking proteins are localized to the tip of motile cilia and might contribute to stabilization of axonemal microtubules (Niwa et al., 2012; Schrøder et al., 2011). Taxol-treated node cilia grew longer, suggesting that hyperstabilization of microtubules might occur at the tip of Taxol-treated node cilia. Super-resolution microscopy might be expected to provide insight into the relation between extension of the axoneme and disorganized arrangement of the doublet microtubules. It has been shown that beating frequency was altered in the zebrafish mutant embryo with shorter cilia in the L-R organizer (Sampaio et al., 2014). However, the length of cilia per se is not responsible for the random directional movement of Taxol-treated node cilia, because node cilia treated with Taxol for a short time (10 min) showed random beating while they retained normal length.

Our data also suggest that correct spatial arrangement of microtubule pairs is essential for stable clockwise rotation of node cilia. However, it remains unknown how the clockwise direction of ciliary rotation is determined. Doublet microtubules are formed from a template in the basal body, which consists of triplet microtubules with established chirality (Li et al., 2012). Given that dynein arms are attached only to A tubules, the clockwise direction of rotation might originate from the chirality of the triplet microtubules in the basal body. The mechanism that determines the chirality of the basal body awaits further study.

EXPERIMENTAL PROCEDURES

Animals

Mice were maintained at the Animal Facility of the Graduate School of Frontier Biosciences, Osaka University, under a 12-h-light, 12-h-dark cycle and were

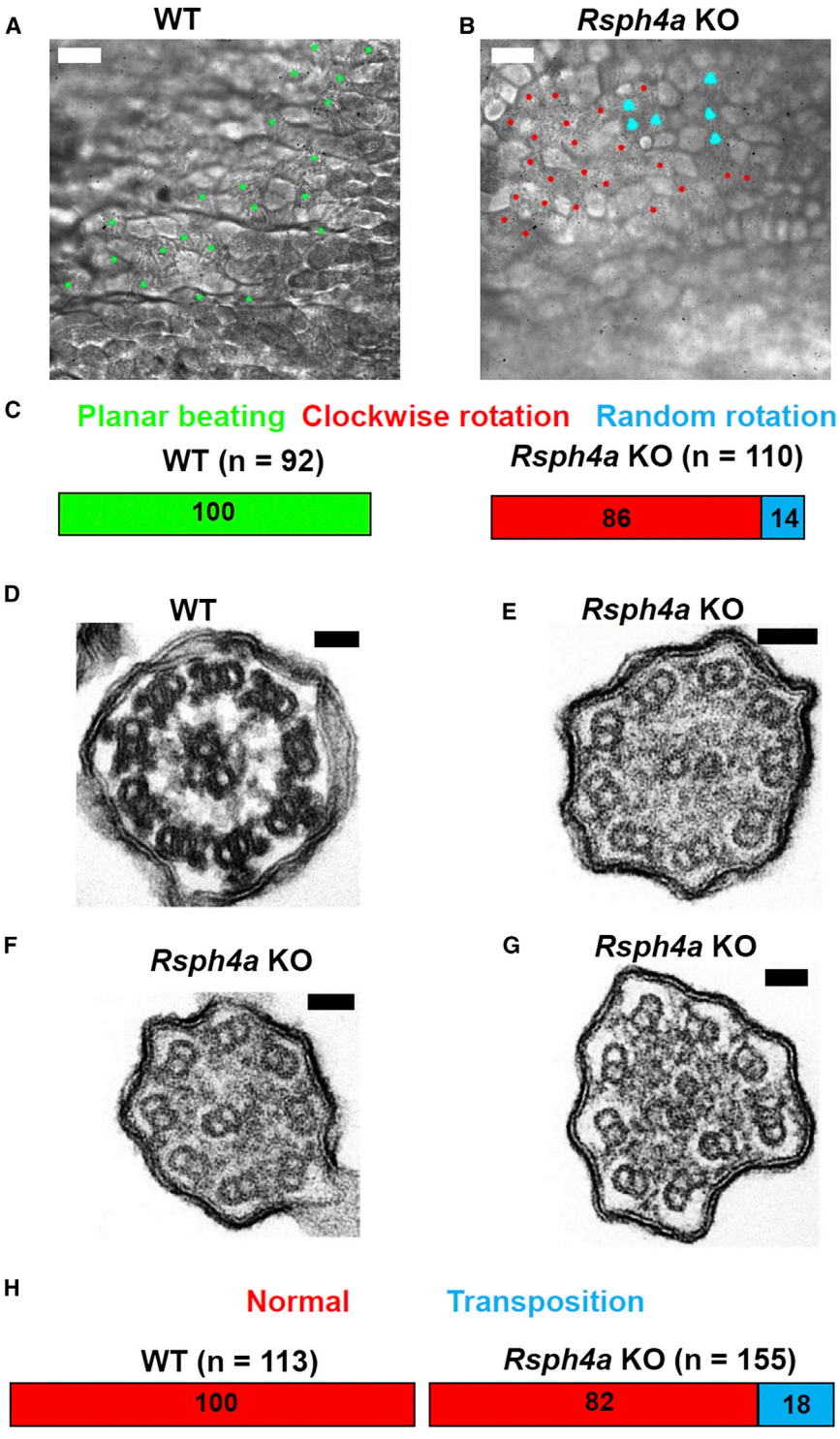

Figure 6. Motion and Structure of Airway Cilia in Radial Spoke Head-Deficient Mice

(A and B) Motion of cilia in airway tissue of WT (A) or *Rsph4a*$^{-/-}$ (knockout, or KO) (B) mice. Green, red, and blue dots denote cilia manifesting planar beating, rotation in a clockwise direction, and rotation in random directions, respectively.

(C) Summary of the motion pattern of airway cilia. Green, red, and blue bars denote the percentages of cilia exhibiting the different motion patterns indicated in (A) and (B).

(D–G) TEM of cross-sections of airway cilia of WT (D) or *Rsph4a*$^{-/-}$ (E–G) mice.

(H) Summary of the arrangement of doublet microtubules in airway cilia. Red and blue bars denote the percentages of cilia showing regular arrangement and transposition of doublet microtubules, respectively.

White and black size bars indicate 10 μm (A and B) and 50 nm (D–G), respectively.

See also Figures S4 and S5.

provided with food and water ad libitum. All experiments were approved by the Institutional Animal Care and Use Committee of Osaka University and under the supervision of Osaka University, approval and license number FBS-12-019. ICR mice were obtained from CLEA Japan.

Generation of *Rsph4a*$^{-/-}$ Mice

A targeting vector for *Rsph4a* was constructed with a design based on flanking LoxP sites (Figure S4). The DNA sequence for a FRT-flanked phosphoglycerate kinase gene (*Pgk*) promoter-driven neomycin resistance gene (*neo*) cassette was positioned between exons 3 and 4, and LoxP sites were introduced to flanking exons 2 and 3. The targeting vector was introduced into embryonic stem (ES) cells, and clones that had undergone homologous recombination were identified by Southern blot analysis and then introduced into ICR early embryos. Chimeric mice were identified on the basis of their coat color, with skin cells derived from the ES clones and ICR cells being black and white. Chimeras with a coat that was 80% to 100% black were crossed with ICR mice, and those showing germline transmission of the modified DNA were mated with CAG-Cre mice (Sakai and Miyazaki, 1997) to generate *Rsph4a*$^{+/-}$ offspring. *Rsph4a*$^{-/-}$ mice and control *Rsph4a*$^{+/+}$ (WT) littermates were generated by intercrossing of *Rsph4a*$^{+/-}$ heterozygotes. PCR primers for detection of the WT allele were 5′-CGAAAGCTTCGCAATAAACA-3′ (P1) and 5′-CAGGGATACGAGGAACCAAA-3′ (P2), and those for detection of the *Rsph4a* knockout allele were 5′-CTCCATGGGCACTTACTTTC-3′ (P3) and P2.

Embryo Dissection and Whole-Embryo Culture

Embryos of timed pregnant ICR female mice were dissected at embryonic day 8 into phenol red-free DMEM supplemented with 10% fetal bovine serum. Dissected embryos were cultured under 5% CO_2 at 37°C in phenol red-free DMEM supplemented with 75% rat serum.

Airway Dissection and Tissue Culture

Airway tissue was dissected from mice at postnatal day 20 and cultured under 5% CO_2 at 37°C in DMEM-Ham's F12 (50:50) supplemented with 1 M HEPES-NaOH (pH 7.2) and 2% fetal bovine serum.

Imaging of Ciliary Motion

The motion of node and airway cilia was visualized with the use of a high-speed point-tracking system (Shinohara et al., 2012). The motion of cilia was thus observed for 5 s (100 frames/s for node cilia and 200 frames/s for airway cilia) with a high-speed CMOS camera (HAS-500M, Detect) that was connected to a

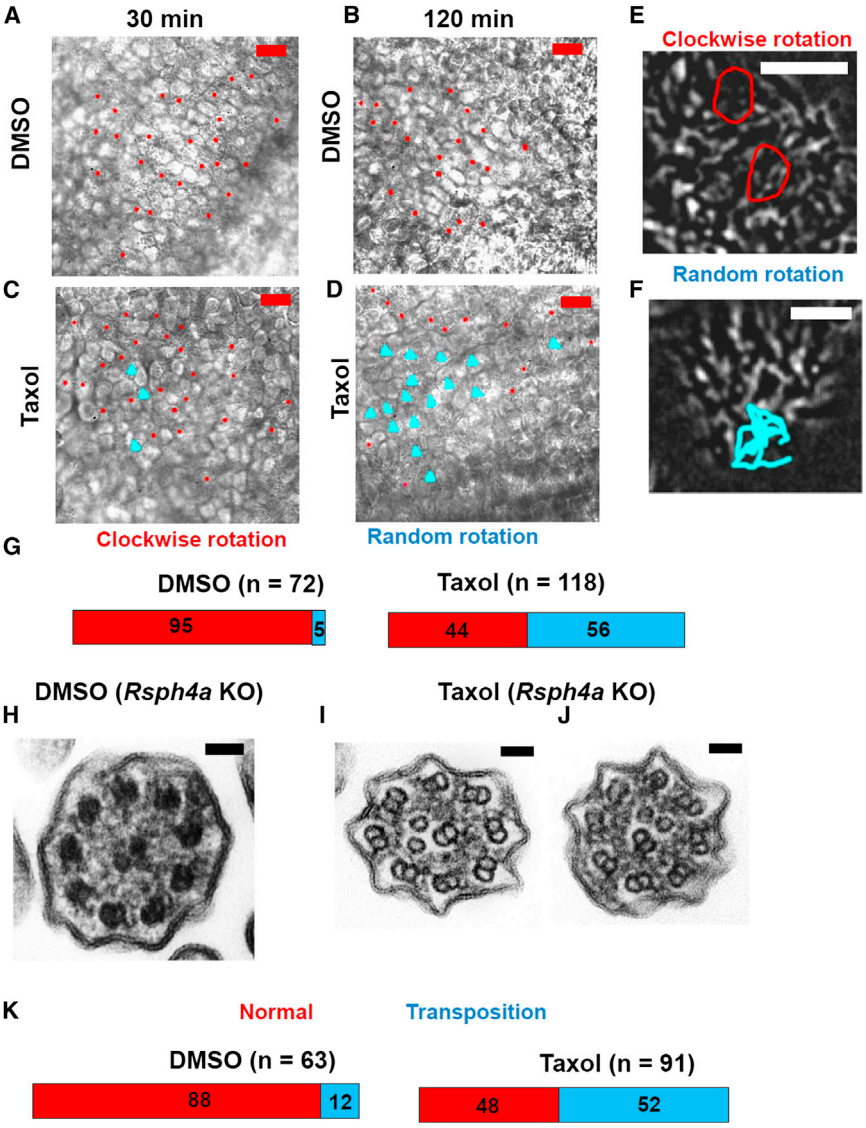

Figure 7. Radial Spokes Maintain Regular Arrangement of Doublet Microtubules in the Face of Perturbation in Mouse Cilia

(A–D) Motion of cilia in airway tissue of *Rsph4a*$^{-/-}$ mice cultured with DMSO or 5 μM Taxol for 30 or 120 min. Red and blue dots denote cilia rotating in a clockwise direction and in random directions, respectively.

(E and F) Traces of ciliary tip rotation in clockwise (E) or random (F) directions.

(G) Summary of the motion pattern for airway cilia of *Rsph4a*$^{-/-}$ mouse tissue treated with DMSO or Taxol for 120 min. Red and blue bars denote the percentages of cilia rotating in clockwise and random directions, respectively.

(H–J) TEM of cross-sections of airway cilia of *Rsph4a*$^{-/-}$ mouse tissue cultured with DMSO or Taxol for 2 hr.

(K) Summary of the arrangement of doublet microtubules for airway cilia treated as in (H)–(J). Red and blue bars denote the percentages of cilia showing regular arrangement and transposition of doublet microtubules, respectively.

Red, white, and black size bars indicate 10 μm (A–D), 5 μm (E and F), and 50 nm (H–J), respectively.

microscope equipped with a 100× oil-immersion objective lens. The specimen was observed with transmitted light from a halogen lamp. Time-series images were captured at a resolution of 1,024 by 992 pixels, with a pixel resolution of 0.082 by 0.082 μm.

Electron Microscopy

For scanning electron microscopy, embryos were observed with a Hitachi S2600-N microscope. For transmission electron microscopy (TEM), embryos were dissected in DMEM supplemented with 25 mM HEPES-NaOH (pH 7.2), fixed for 5 hr at room temperature with 2% paraformaldehyde and 2.5% glutaraldehyde in 0.1 M cacodylate buffer (pH 7.4), rinsed with 0.1 M cacodylate buffer, exposed to 2% OsO_4 in 0.1 M cacodylate buffer for 1 hr on ice, dehydrated in a graded series of ethanol solutions and QY-1, and embedded in Quetol 812 (Nisshin EM). Ultrathin sections were cut with the use of an Ultramicrotome (Reichert-Jung Ultracut E), stained with uranyl acetate and lead (by Sato's method), and examined with a JEM 1200-EX or JEM 1400Plus microscope (JEOL) at an acceleration voltage of 80 or 100 kV.

Electron Tomography with an Ultra-High-Voltage Electron Microscope

For observation by ultra-high-voltage electron microscopic tomography, sections were cut at a thickness of 1,000 nm and mounted on Formvar-coated 75-mesh molybdenum grids. The sections, with colloidal gold particles (20 nm) deposited on both surfaces, were observed with an ultra-high-voltage electron microscope (H-3000, Hitachi) operating at 2 MeV. Images were acquired at a magnification of 20,000× from −60° to +60° at 2° intervals around a single-axis tilt series and were recorded with a 4,096 by 4,096 F415S slow-scan charge-coupled device camera with a pixel size of 15 μm (TVIPS). Image alignment, three-dimensional reconstruction, and modeling were performed with the IMOD image-processing package (Kremer et al., 1996).

Computer Simulation of the Motion of Node Cilia

The three-dimensional ultrastructure of a control cilium and four Taxol-treated cilia was revealed by electron tomography. We constructed mesh frameworks for computer simulation based on the electron tomography data. The image datasets were processed with an open-source suite of modeling software (IMOD 4.5) to extract the center line of each microtubule doublet and the shape of the ciliary surface. The geometry of the ciliary ultrastructure was then reconstructed with a mesh generator (CFD-GEOM, ESI Group). For details, see Supplemental Experimental Procedures.

SUPPLEMENTAL INFORMATION

Supplemental Information includes Supplemental Experimental Procedures, five figures, and six movies and can be found with this article online at http://dx.doi.org/10.1016/j.devcel.2015.10.001.

AUTHOR CONTRIBUTIONS

K.S. and H.H. designed and performed the experiments and generated knockout mice. D.C. performed computer simulation based on experimental data. T.N. performed analysis of electron tomography. K.M. and S.Y. prepared TEM samples. K.S., D.C., and H.H. wrote the paper.

ACKNOWLEDGMENTS

We thank C. Brokaw, F. Jülicher, Y. Okada, T. Yagi, and K. Oiwa for discussion on modeling of cilia, cilia-driven fluid flow, and dynein arms of cilia; T. Hasegawa, Y. Muranaka, and R. Kuwahara for preparation of TEM samples; Y. Ventikos for support of computer simulation; and S. Tsukita, A. Fukumoto, H. Nishimura, Y. Ikawa, K. Ohnishi, and K. Suzuki for technical assistance. D.C. is supported by the National Natural Science Foundation of China (31200704 and 81471752). This work was supported by CREST, the Japan Science and Technology Corporation (JST), a Grant-in-Aid for Young Scientists (Project No. 24770209), the Japan Society for the Promotion of Science (JSPS), and the Nanotechnology Platform (Project No. 12024046) of the Ministry of Education, Culture, Sports, Science, and Technology (MEXT) of Japan. Requests for the mice described in this paper should be addressed to H.H.

Received: June 1, 2015
Revised: August 29, 2015
Accepted: October 1, 2015
Published: October 26, 2015

REFERENCES

Antony, D., Becker-Heck, A., Zariwala, M.A., Schmidts, M., Onoufriadis, A., Forouhan, M., Wilson, R., Taylor-Cox, T., Dewar, A., Jackson, C., et al. (2013). Mutations in CCDC39 and CCDC40 are the major cause of primary ciliary dyskinesia with axonemal disorganization and absent inner dynein arms. Hum. Mutat. *34*, 462–472.

Becker-Heck, A., Zohn, I.E., Okabe, N., Pollock, A., Lenhart, K.B., Sullivan-Brown, J., McSheene, J., Loges, N.T., Olbrich, H., Haeffner, K., et al. (2011). The coiled-coil domain containing protein CCDC40 is essential for motile cilia function and left-right axis formation. Nat. Genet. *43*, 79–84.

Boisvieux-Ulrich, E., Laine, M.C., and Sandoz, D. (1989). In vitro effects of Taxol on ciliogenesis in quail oviduct. J. Cell Sci. *92*, 9–20.

Brokaw, C.J. (2002). Computer simulation of flagellar movement VIII: coordination of dynein by local curvature control can generate helical bending waves. Cell Motil. Cytoskeleton *53*, 103–124.

Brokaw, C.J. (2005). Computer simulation of flagellar movement IX. Oscillation and symmetry breaking in a model for short flagella and nodal cilia. Cell Motil. Cytoskeleton *60*, 35–47.

Brokaw, C.J. (2009). Thinking about flagellar oscillation. Cell Motil. Cytoskeleton *66*, 425–436.

Burgoyne, T., Lewis, A., Dewar, A., Luther, P., Hogg, C., Shoemark, A., and Dixon, M. (2014). Characterizing the ultrastructure of primary ciliary dyskinesia transposition defect using electron tomography. Cytoskeleton (Hoboken) *71*, 294–301.

Cartwright, J.H.E., Piro, O., and Tuval, I. (2004). Fluid-dynamical basis of the embryonic development of left-right asymmetry in vertebrates. Proc. Natl. Acad. Sci. USA *101*, 7234–7239.

Castleman, V.H., Romio, L., Chodhari, R., Hirst, R.A., de Castro, S.C.P., Parker, K.A., Ybot-Gonzalez, P., Emes, R.D., Wilson, S.W., Wallis, C., et al. (2009). Mutations in radial spoke head protein genes RSPH9 and RSPH4A cause primary ciliary dyskinesia with central-microtubular-pair abnormalities. Am. J. Hum. Genet. *84*, 197–209.

Chen, D., Norris, D., and Ventikos, Y. (2011). Ciliary behaviour and mechanotransduction in the embryonic node: computational testing of hypotheses. Med. Eng. Phys. *33*, 857–867.

Chen, D., Zhong, Y., Shinohara, K., Nishida, T., Hasegawa, T., and Hamada, H. (2014). The dynein-triggered ciliary motion in embryonic nodes: an exploratory study based on computational models. Biomed. Mater. Eng. *24*, 2495–2501.

Chilvers, M.A., Rutman, A., and O'Callaghan, C. (2003). Ciliary beat pattern is associated with specific ultrastructural defects in primary ciliary dyskinesia. J. Allergy Clin. Immunol. *112*, 518–524.

Feistel, K., and Blum, M. (2006). Three types of cilia including a novel 9+4 axoneme on the notochordal plate of the rabbit embryo. Dev. Dyn. *235*, 3348–3358.

Ferrante, M.I., Romio, L., Castro, S., Collins, J.E., Goulding, D.A., Stemple, D.L., Woolf, A.S., and Wilson, S.W. (2009). Convergent extension movements and ciliary function are mediated by ofd1, a zebrafish orthologue of the human oral-facial-digital type 1 syndrome gene. Hum. Mol. Genet. *18*, 289–303.

Fox, L.A., and Sale, W.S. (1987). Direction of force generated by the inner row of dynein arms on flagellar microtubules. J. Cell Biol. *105*, 1781–1787.

Gardner, L.C., O'Toole, E., Perrone, C.A., Giddings, T., and Porter, M.E. (1994). Components of a "dynein regulatory complex" are located at the junction between the radial spokes and the dynein arms in *Chlamydomonas* flagella. J. Cell Biol. *127*, 1311–1325.

Hashimoto, M., Shinohara, K., Wang, J., Ikeuchi, S., Yoshiba, S., Meno, C., Nonaka, S., Takada, S., Hatta, K., Wynshaw-Boris, A., and Hamada, H. (2010). Planar polarization of node cells determines the rotational axis of node cilia. Nat. Cell Biol. *12*, 170–176.

Heuser, T., Raytchev, M., Krell, J., Porter, M.E., and Nicastro, D. (2009). The dynein regulatory complex is the nexin link and a major regulatory node in cilia and flagella. J. Cell Biol. *187*, 921–933.

Hilfinger, A., and Jülicher, F. (2008). The chirality of ciliary beats. Phys. Biol. *5*, 016003.

Hirokawa, N., Tanaka, Y., Okada, Y., and Takeda, S. (2006). Nodal flow and the generation of left-right asymmetry. Cell *125*, 33–45.

Kinzel, D., Boldt, K., Davis, E.E., Burtscher, I., Trümbach, D., Diplas, B., Attié-Bitach, T., Wurst, W., Katsanis, N., Ueffing, M., and Lickert, H. (2010). Pitchfork regulates primary cilia disassembly and left-right asymmetry. Dev. Cell *19*, 66–77.

Knowles, M.R., Ostrowski, L.E., Leigh, M.W., Sears, P.R., Davis, S.D., Wolf, W.E., Hazucha, M.J., Carson, J.L., Olivier, K.N., Sagel, S.D., et al. (2014). Mutations in RSPH1 cause primary ciliary dyskinesia with a unique clinical and ciliary phenotype. Am. J. Respir. Crit. Care Med. *189*, 707–717.

Kramer-Zucker, A.G., Olale, F., Haycraft, C.J., Yoder, B.K., Schier, A.F., and Drummond, I.A. (2005). Cilia-driven fluid flow in the zebrafish pronephros, brain and Kupffer's vesicle is required for normal organogenesis. Development *132*, 1907–1921.

Kremer, J.R., Mastronarde, D.N., and McIntosh, J.R. (1996). Computer visualization of three-dimensional image data using IMOD. J. Struct. Biol. *116*, 71–76.

Kunimoto, K., Yamazaki, Y., Nishida, T., Shinohara, K., Ishikawa, H., Hasegawa, T., Okanoue, T., Hamada, H., Noda, T., Tamura, A., et al. (2012). Coordinated ciliary beating requires Odf2-mediated polarization of basal bodies via basal feet. Cell *148*, 189–200.

Lechtreck, K.F., Delmotte, P., Robinson, M.L., Sanderson, M.J., and Witman, G.B. (2008). Mutations in Hydin impair ciliary motility in mice. J. Cell Biol. *180*, 633–643.

Li, S., Fernandez, J.J., Marshall, W.F., and Agard, D.A. (2012). Three-dimensional structure of basal body triplet revealed by electron cryo-tomography. EMBO J. *31*, 552–562.

Lin, J., Yin, W., Smith, M.C., Song, K., Leigh, M.W., Zariwala, M.A., Knowles, M.R., Ostrowski, L.E., and Nicastro, D. (2014). Cryo-electron tomography reveals ciliary defects underlying human RSPH1 primary ciliary dyskinesia. Nat. Commun. *5*, 5727.

Lindemann, C.B. (1994). A "geometric clutch" hypothesis to explain oscillations of the axoneme of cilia and flagella. J. Theor. Biol. *168*, 175–189.

Lindemann, C.B. (2003). Structural-functional relationships of the dynein, spokes, and central-pair projections predicted from an analysis of the forces acting within a flagellum. Biophys. J. *84*, 4115–4126.

Lindemann, C.B., Macauley, L.J., and Lesich, K.A. (2005). The counterbend phenomenon in dynein-disabled rat sperm flagella and what it reveals about the interdoublet elasticity. Biophys. J. *89*, 1165–1174.

McGrath, J., Somlo, S., Makova, S., Tian, X., and Brueckner, M. (2003). Two populations of node monocilia initiate left-right asymmetry in the mouse. Cell *114*, 61–73.

Merveille, A.C., Davis, E.E., Becker-Heck, A., Legendre, M., Amirav, I., Bataille, G., Belmont, J., Beydon, N., Billen, F., Clément, A., et al. (2011). CCDC39 is

required for assembly of inner dynein arms and the dynein regulatory complex and for normal ciliary motility in humans and dogs. Nat. Genet. *43*, 72–78.

Nakamura, T., and Hamada, H. (2012). Left-right patterning: conserved and divergent mechanisms. Development *139*, 3257–3262.

Nicastro, D., Schwartz, C., Pierson, J., Gaudette, R., Porter, M.E., and McIntosh, J.R. (2006). The molecular architecture of axonemes revealed by cryoelectron tomography. Science *313*, 944–948.

Niwa, S., Nakajima, K., Miki, H., Minato, Y., Wang, D., and Hirokawa, N. (2012). KIF19A is a microtubule-depolymerizing kinesin for ciliary length control. Dev. Cell *23*, 1167–1175.

Nogales, E., Wolf, S.G., and Downing, K.H. (1998). Structure of the α β tubulin dimer by electron crystallography. Nature *391*, 199–203.

Nonaka, S., Tanaka, Y., Okada, Y., Takeda, S., Harada, A., Kanai, Y., Kido, M., and Hirokawa, N. (1998). Randomization of left-right asymmetry due to loss of nodal cilia generating leftward flow of extraembryonic fluid in mice lacking KIF3B motor protein. Cell *95*, 829–837.

Nonaka, S., Yoshiba, S., Watanabe, D., Ikeuchi, S., Goto, T., Marshall, W.F., and Hamada, H. (2005). De novo formation of left-right asymmetry by posterior tilt of nodal cilia. PLoS Biol. *3*, e268.

Oda, T., Yanagisawa, H., Yagi, T., and Kikkawa, M. (2014). Mechanosignaling between central apparatus and radial spokes controls axonemal dynein activity. J. Cell Biol. *204*, 807–819.

Okada, Y., Takeda, S., Tanaka, Y., Izpisúa Belmonte, J.C., and Hirokawa, N. (2005). Mechanism of nodal flow: a conserved symmetry breaking event in left-right axis determination. Cell *121*, 633–644.

Omran, H., Kobayashi, D., Olbrich, H., Tsukahara, T., Loges, N.T., Hagiwara, H., Zhang, Q., Leblond, G., O'Toole, E., Hara, C., et al. (2008). Ktu/PF13 is required for cytoplasmic pre-assembly of axonemal dyneins. Nature *456*, 611–616.

Onoufriadis, A., Shoemark, A., Schmidts, M., Patel, M., Jimenez, G., Liu, H., Thomas, B., Dixon, M., Hirst, R.A., Rutman, A., et al.; UK10K (2014). Targeted NGS gene panel identifies mutations in RSPH1 causing primary ciliary dyskinesia and a common mechanism for ciliary central pair agenesis due to radial spoke defects. Hum. Mol. Genet. *23*, 3362–3374.

Pigino, G., Bui, K.H., Maheshwari, A., Lupetti, P., Diener, D., and Ishikawa, T. (2011). Cryoelectron tomography of radial spokes in cilia and flagella. J. Cell Biol. *195*, 673–687.

Sakai, K., and Miyazaki, Ji. (1997). A transgenic mouse line that retains Cre recombinase activity in mature oocytes irrespective of the cre transgene transmission. Biochem. Biophys. Res. Commun. *237*, 318–324.

Sampaio, P., Ferreira, R.R., Guerrero, A., Pintado, P., Tavares, B., Amaro, J., Smith, A.A., Montenegro-Johnson, T., Smith, D.J., and Lopes, S.S. (2014). Left-right organizer flow dynamics: how much cilia activity reliably yields laterality? Dev. Cell *29*, 716–728.

Satir, P., Heuser, T., and Sale, W.S. (2014). A structural basis for How motile cilia beat. Bioscience *64*, 1073–1083.

Schrøder, J.M., Larsen, J., Komarova, Y., Akhmanova, A., Thorsteinsson, R.I., Grigoriev, I., Manguso, R., Christensen, S.T., Pedersen, S.F., Geimer, S., and Pedersen, L.B. (2011). EB1 and EB3 promote cilia biogenesis by several centrosome-related mechanisms. J. Cell Sci. *124*, 2539–2551.

Sharma, N., Kosan, Z.A., Stallworth, J.E., Berbari, N.F., and Yoder, B.K. (2011). Soluble levels of cytosolic tubulin regulate ciliary length control. Mol. Biol. Cell *22*, 806–816.

Shinohara, K., Kawasumi, A., Takamatsu, A., Yoshiba, S., Botilde, Y., Motoyama, N., Reith, W., Durand, B., Shiratori, H., and Hamada, H. (2012). Two rotating cilia in the node cavity are sufficient to break left–right symmetry in the mouse embryo. Nat. Commun. *3*, 622.

Smith, E.F., and Yang, P. (2004). The radial spokes and central apparatus: mechano-chemical transducers that regulate flagellar motility. Cell Motil. Cytoskeleton *57*, 8–17.

Song, H., Hu, J., Chen, W., Elliott, G., Andre, P., Gao, B., and Yang, Y. (2010). Planar cell polarity breaks bilateral symmetry by controlling ciliary positioning. Nature *466*, 378–382.

Summers, K.E., and Gibbons, I.R. (1971). Adenosine triphosphate-induced sliding of tubules in trypsin-treated flagella of sea-urchin sperm. Proc. Natl. Acad. Sci. USA *68*, 3092–3096.

Tabin, C.J., and Vogan, K.J. (2003). A two-cilia model for vertebrate left-right axis specification. Genes Dev. *17*, 1–6.

Takada, S., and Kamiya, R. (1994). Functional reconstitution of *Chlamydomonas* outer dynein arms from α-β and γ subunits: requirement of a third factor. J. Cell Biol. *126*, 737–745.

Tanaka, Y., Okada, Y., and Hirokawa, N. (2005). FGF-induced vesicular release of Sonic hedgehog and retinoic acid in leftward nodal flow is critical for left-right determination. Nature *435*, 172–177.

Ueno, H., Ishikawa, T., Bui, K.H., Gonda, K., Ishikawa, T., and Yamaguchi, T. (2012). Mouse respiratory cilia with the asymmetric axonemal structure on sparsely distributed ciliary cells can generate overall directional flow. Nanomedicine (Lond.) *8*, 1081–1087.

Woolley, D.M. (1997). Studies on the eel sperm flagellum. I. The structure of the inner dynein arm complex. J. Cell Sci. *110*, 85–94.

Woolley, D.M. (1998). Studies on the eel sperm flagellum. 3. Vibratile motility and rotatory bending. Cell Motil. Cytoskeleton *39*, 246–255.